# 3.4 AUTOMATED TWO-HOUR THUNDERSTORM GUIDANCE FORECASTS

Jerome P. Charba*
Feng Liang
Meteorological Development Laboratory
Office of Science and Technology
National Weather Service
Silver Spring, Maryland

## 1. INTRODUCTION

Thunderstorms account for a large percentage of the air traffic delays, especially during the warm season. The National Weather Service (NWS) provides air traffic managers with various automated and manual convective forecast products for tactical and strategical aviation operations. Still, great benefits to the air transportation industry could be reaped from improvements in the accuracy and resolution in thunderstorm forecasts.

The Meteorological Development Laboratory (MDL) [formerly Techniques Development Laboratory (TDL)] of the NWS has provided automated statistically-based thunderstorm guidance forecasts since the early 1970s (Alaka et al. 1973). Over the years, most of this guidance has been based on the MOS approach (Glahn and Lowry 1972). One exception was a very short range (2-6 h) thunderstorm product (Charba 1977), which made heavy use of recent observational data, in addition to numerical model output. More recent MDL guidance products under 24 hours have been based on the Localized Aviation MOS Program (LAMP) approach (Glahn and Unger 1986; Charba 1998; Glahn and Ghirardelli 2004). In this approach, MOS forecasts issued two or four times daily are updated hourly, based on the latest observational data. This article describes how LAMP is being applied to update a new MOS thunderstorm product, with higher spatial and temporal resolution than previously available (Hughes 2004).

## 2. PREDICTAND

The thunderstorm predictand is defined as the occurrence or non-occurrence of one or more cloud-to-ground (CTG) lightning strikes in a 2-h period in a 20-km gridbox. The CTG lightning data are from the National Lightning Detection Network (NLDN; Cummins et al.1998). The geographical coverage of the thunderstorm gridboxes is shown in Fig. 1; the grid is compatible with that used for the National Digital Forecast Database (NDFD) of the NWS (Glahn and Ruth 2003). [Coverage outside the continental United States (CONUS) is not presently possible because a sufficient lightning database does not exist there.]

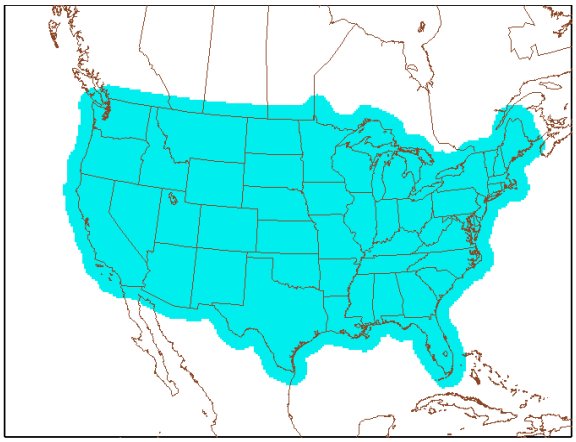

**Figure 1**. Thunderstorm forecast coverage, which extends 150 km beyond CONUS boundaries.

When fully implemented, the product will be issued hourly for 0-2, 2-4, … , and 22-24 h projections. The basic form of the forecasts is probability, but a categorical form will also be provided. The categorical forecasts are derived by applying objectively-specified thresholds to the probabilities.

## 3. PREDICTORS

The thunderstorm predictors were derived from multiple inputs, which include radar reflectivity measurements, CTG lightning reports, METAR observations, thunderstorm climatology, and topography, in addition to the MOS forecasts. The derivation of the predictors involves data quality control, various types of processing and analyses, and the application of advective models. The fol-

* *Corresponding author address:*
Jerome P. Charba, National Weather Service
1325 East West Highway, Room 10410
Silver Spring, MD 20910-3283
email: jerome.charba@noaa.gov

lowing sub-sections provide brief summaries of the predictor development.

### *3.1 Radar Reflectivity and Lightning Strike Data*

Quality-controlled radar reflectivity data on a 10-km grid were used to specify the maximum and mean reflectivities in 20-km gridboxes . (Charba and Feng 2005 discuss the source of the reflectivity data and the multiple quality control processes applied to remove non-precipitation echoes.) Heavy spatial smoothing was then applied to the 20-km grids to obtain the predictor fields, as it was found the raw field contains no predictive information beyond that contained in the smoothed field. Fig. 2 shows an example of the smoothing for the maximum reflectivity field. Similar predictor variables were derived from 1-h CTG lighting strike counts in 10-km gridboxes that are identical to those of the base radar reflectivity grids.

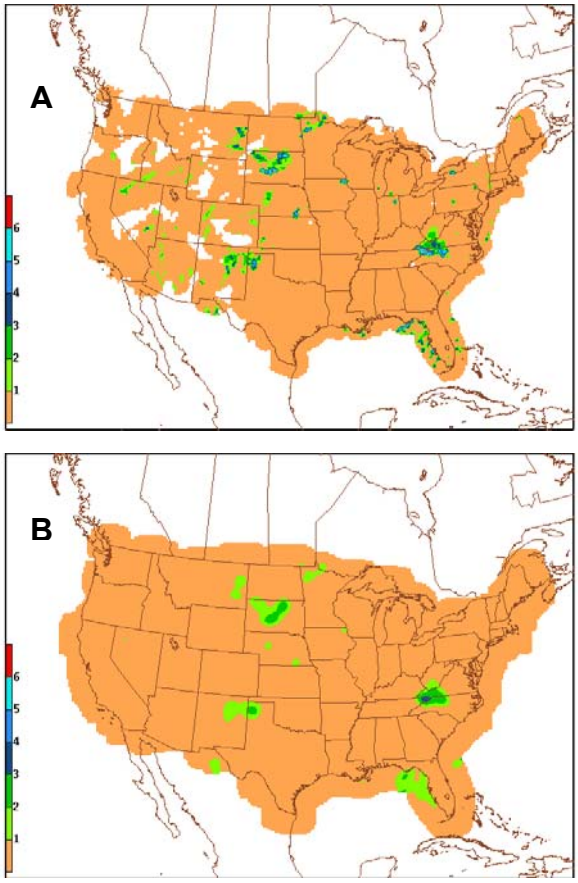


**Figure 2**. Maximum radar reflectivity in 20-km gridboxes advected 3 hours from 0900 UTC, 27 July 1997 in (a) raw and (b) smoothed forms. The smoother extrapolates into missing data (white) areas in (a). The reflectivity categories are: < 1 = <15 dbZ; 1 = 15–30 dbZ; 2 = 30–40 dbZ; 3 = 40–45 dbZ; 4 = 45–50 dbZ; 5 = 50-55 dbZ; 6 = ≥55 dbZ.

### *3.2 Thunderstorm Climatology*

Monthly relative frequencies (RF) of the thunderstorm predictand for each 2-h period of the day were derived from a 10-year sample (1994-2003). An example RF field is shown in Fig. 3a. Due to the shortness of the sample, the raw RFs do not represent true climatic values, especially where the values are near zero. Thus, weighted three-point averaging of the gridpoint values in four dimensions was used to smooth the raw fields (Fig. 3b). The amount of smoothing applied for each of the two time dimensions (period-to-period and month-to-month) and the two grid dimensions was minimized to maximize detail in the smoothed grids.

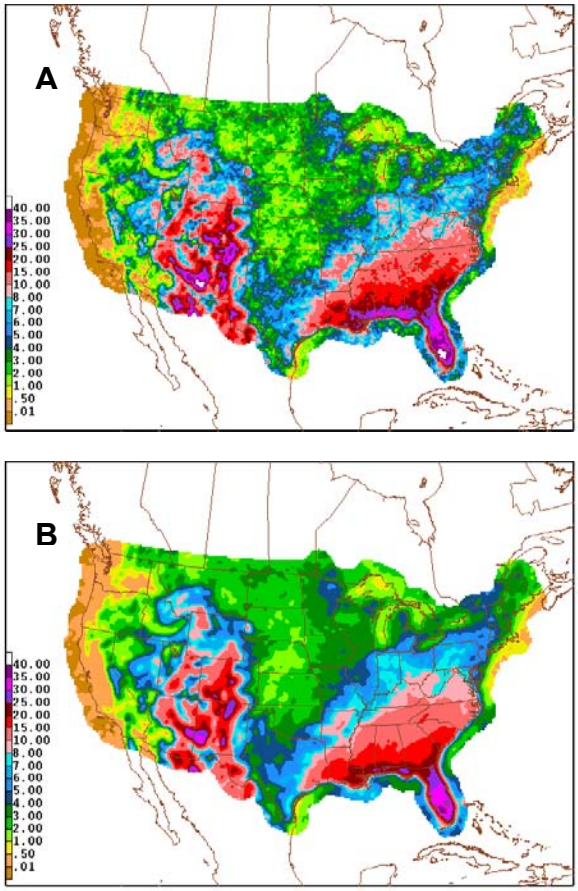


**Figure 3**. July relative frequency (%) of the thunderstorm predictand for 2000 – 2200 UTC in (a) raw and (b) smoothed forms.

Effective use of the smoothed RF as a thunderstorm predictor is made by combining it with a relatively strong predictor of thunderstorms. Specifically, it is applied as a product of itself and the MOS thunderstorm probability input. In this product, the current MOS probability instills day-to-day variations to an otherwise environmentally-ignorant climatological variable.

### *3.3 METAR Observations, Topography, and Model Forecasts*

METAR observations, topography, and a few forecast fields from the National Centers for Environmental Prediction (NCEP) Global Forecast System (GFS; Iredell and Caplan 1997) were used together to derive selected fields thought to be useful as thunderstorm predictors. METAR observations of surface wind components, temperature, dew point etc. were objectively analyzed to an 80-km grid (Glahn and Ghirardelli 2004). The topography, which was derived from 1-km ground elevations from the U.S. Geological Survey, was used mainly for computing fine-scale, terrain-forced vertical velocity (TVV). The small number of forecast fields from the GFS was for the derivation of predictors not included in the MOS thunderstorm regression equations. Examples are forecasts of surface winds used to compute TVV and surface moisture divergence, and 500-mb temperature forecasts used to compute surface-based convective instability indices.

### *3.4 Advective Models*

Several advective models are applied to produce 1- to 24-h forecasts for all gridded observational variables embodied in the LAMP system (Glahn and Unger 1986). The model used to advect the radar and lightning fields was especially useful because the advection extends the predictive value of these variables well beyond that obtained from the initial fields. Small predictor contributions result from forecasts from the sea level pressure and saturation deficit models.

### *3.5 MOS Probability Forecasts*

Newly-developed MOS thunderstorm probability forecasts on the same 20-km grid as for LAMP are used as a major predictor input. The MOS thunderstorm probabilities, which are based on the NCEP GFS and will be produced four times daily (Hughes 2004), are defined identically to those for LAMP, except they apply to a 3-h period rather than to 2 hours. In the LAMP application, the MOS probabilities are smoothed with a 1-2-1 smoother to remove fine scale variability, and some forecast periods are time-interpolated to better match the LAMP periods. In the next section, we show how LAMP predictors effectively update the MOS forecasts, especially at early LAMP forecast projections.

## 4. REGRESSION EQUATIONS

### *4.1 Equation Development*

The regression equations are derived separately for each of the 13 geographical regions shown in Fig. 4. The regions were drawn subjectively, with guidance from the LAMP thunderstorm climatology fields.

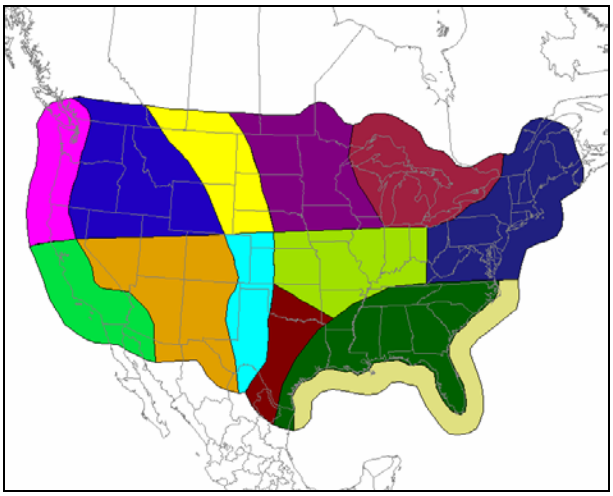

**Figure 4**. Geographical regions used for deriving the regression equations.

Six years of historical data (1998-2003) are presently used for experimental development of the regression equations. This substantial sample allows for seasonal stratification of the equations, with separate equations for the summer (1 July – 15 October), cool (16 October – 31 March), and spring (1 April – 30 June) periods. Also, separate equations are developed for each hour of the day.

At this point, we are in the beginning stages of the equation development. Experimental equations have been developed for the summer for one hourly cycle time, with tests of a few additional candidate predictors still pending. Despite the limited equation development to date, we expect the predominant predictor properties exhibited the experimental equations to be retained in the final

equations. Thus, a brief examination of the predictor properties is presented.

### *4.2 Predictor Ranking*

One approach used to assess the contribution of the various predictors in the regression equations was to examine their order of selection in the screening regression process. Predictors selected earliest have greatest contributions to the forecast probabilities because they explain the most predictand variance. It was found the observed and advected lightning variables ranked first, the MOS thunderstorm forecasts second, observed and advected radar variables third (the low overall ranking is due partly to the strong correlation with the lightning variables), and thunderstorm climatology last. It should be noted these rankings are based on all LAMP forecast projections combined. When a lightning predictor (or a radar predictor) was selected first, the predictand variance explained was invariably for the shortest forecast projection.

### *4.3 Example Forecast*

Another approach used to assess the impact of predictors in the regression equations was to compare the forecast probability fields with predictor fields in cases selected from the (independent) 1997 season. Fig. 5 shows the 1-3 h LAMP thunderstorm probability from the 0900 UTC data observation time on 27 July 1997, together with two dominant predictor fields. Note that the advected lightning count (Fig. 5b) and MOS probability predictors (Fig. 5c) are strongly reflected in the LAMP forecast (Fig. 5a). Also note that the 2-h LAMP forecast contains greater spatial detail and higher peak probabilities than the 3-h MOS forecast. Further, the detail in the LAMP forecast corresponds well with the reported lightning count pattern (Fig. 5d). On the other hand, the correspond-

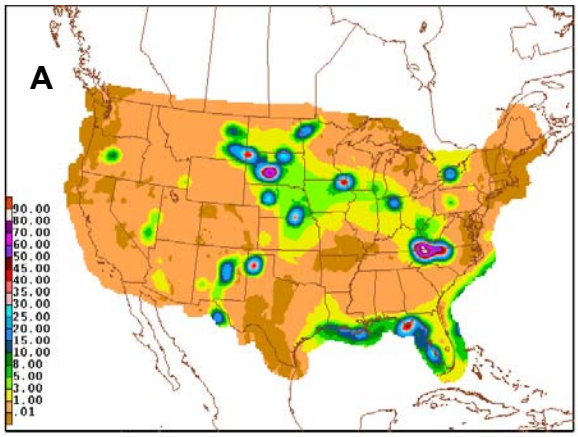


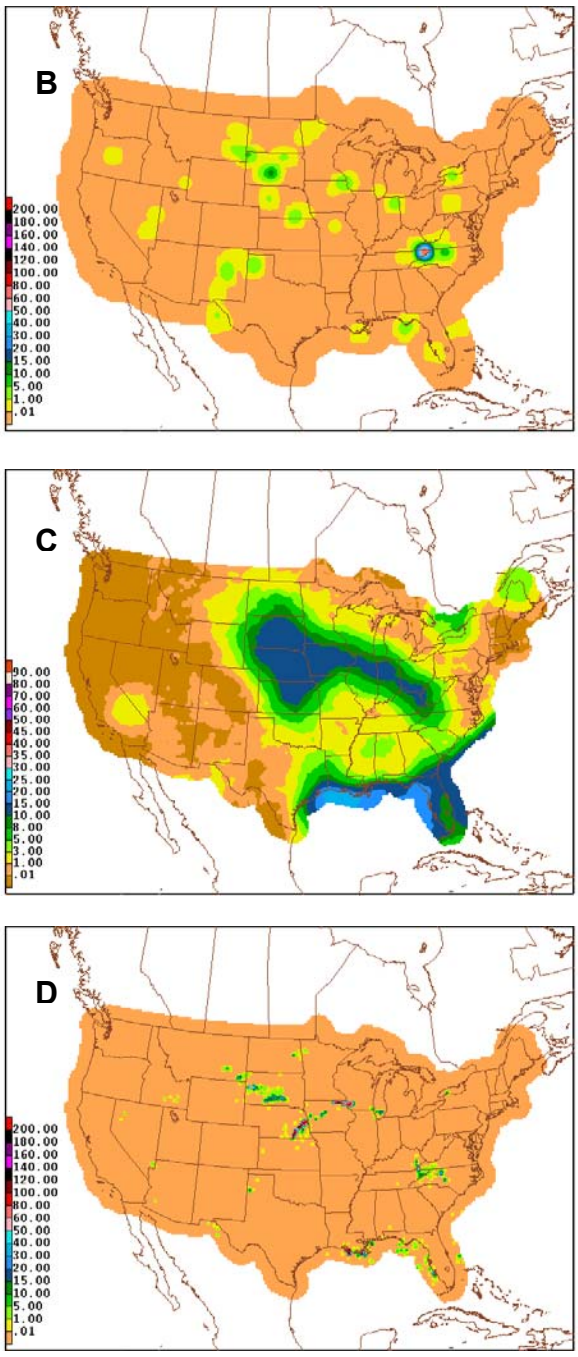


**Figure 5.** For 27 July 1997, (a) 1-3 h LAMP thunderstorm probability (%) forecast and (b) 1-h lightning count advected 3 hours from 0900 UTC, (c) 9-12 h MOS thunderstorm probability (%) forecast from 0000 UTC, and (d) the observed lightning count in 20-km gridboxes for the LAMP forecast valid period.

ing 11-13 h LAMP forecast (Fig. 6a) is quite similar to the 19-22 h (time-interpolated) MOS forecast (Fig. 6b). Also, the peak LAMP probabilities are almost the same as the peak MOS values. Thus, we see that the updating capability of LAMP is strong at the shortest forecast projection and relatively weak at the longer projection.

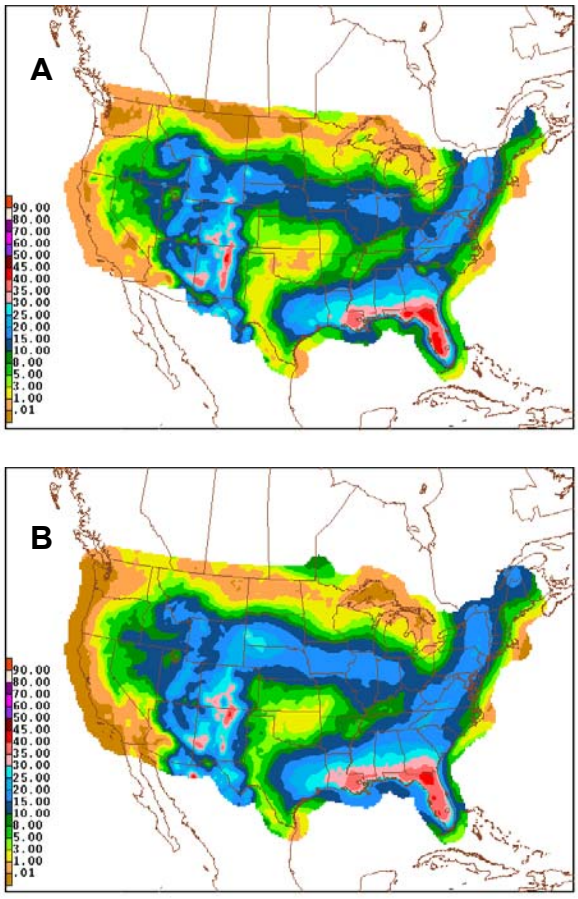


**Figure 6**. (a) 11-13 h LAMP thunderstorm probability (%) from 0900 UTC and (b) 19-22 h (time-interpolated) MOS thunderstorm probability (%) from 0000 UTC on 27 July 1997.

## 5. FORECAST PERFORMANCE

A useful objective measure of forecast skill for the LAMP probability forecasts is the improvement in Brier Score (Brier 1950) over the MOS forecast input. The MOS forecast as a performance benchmark is meaningful, in part because Hughes (2004) has already shown the MOS thunderstorm forecasts are skillful relative to thunderstorm climatology. Thus, the improvement over MOS specifically measures the updating effectiveness of LAMP.

Before the LAMP forecasts could be comparatively scored against MOS, it was necessary to recalibrate the MOS probabilities from their 3-h valid period to the LAMP 2-h period. This was done by deriving calibrated MOS (CMOS) regression equations, wherein the LAMP 2-h predictand was regressed, with the MOS thunderstorm probability as the sole predictor. The probabilities from the CMOS equations were then used in the comparative verification with LAMP. The validity of this approach was demonstrated in an experiment wherein special MOS regression equations with 2-h valid periods were developed using the same predictors as those for the 3-h MOS equations. In comparison tests of the 2-h CMOS probabilities with the 2-h MOS probabilities, it was found the two sets of forecasts were essentially identical.

The Brier Score improvement of LAMP over CMOS as a function of LAMP projection from 0900 UTC during the 1997 summer is shown in Fig. 7. As before, the MOS forecasts are from the 0000 UTC cycle, so 9 hours must be added to obtain their projections. The independent sample is composed of all days of the 1997 summer and all gridpoints within the CONUS. The sample sizes range from 2,381,731 cases at the 3-h projection to 1,835,161 cases at the 25-h projection. The reduction in sample size with increasing projection results from the advection of radar and lightning data coverage boundaries into the forecast area.

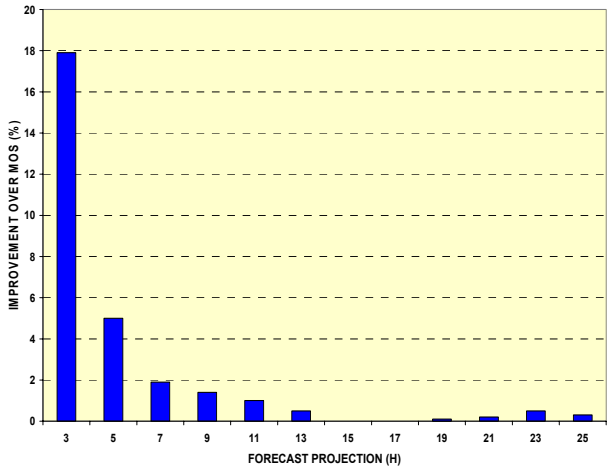


**Figure 7**. Brier Score improvement (%) of LAMP over MOS as a function of LAMP forecast projection for the 1997 summer. The forecast projections are relative to the 0900 UTC LAMP cycle; the MOS forecasts are from the 0000 UTC cycle.

Fig. 7 shows the benefit of the LAMP updating was substantial at the 3-h projection, but the benefit decreased sharply with increasing projection. Specifically, the LAMP improvement of about 18% at the 3-h projection decreases to zero by 15 hours and rises only slightly thereafter.

## 6. REMARKS AND PLANS

With the completion in the near future of the 0900 UTC LAMP development for the summer season, only small improvements in the results presented here are expected. However, as subsequent efforts turn to other cycles and seasons, substantial improvements in the results may occur. This optimism rests on the belief that the combination of 0900 UTC LAMP cycle and summer season may be among the most challenging for LAMP to yield significant updating value. The reason is that predictive information derived from observational fields may be minimal at this early morning hour for the summer season.

We expect to begin experimental production of the LAMP thunderstorm forecasts over the CONUS in real time in late 2005. The probability and categorical forecasts will be produced on NCEP's mainframe computer and likely made available on the internet.

## 7. ACKOWLEDGEMENTS

We acknowledge the contribution of many members of MDL to the MOS and LAMP development systems. Specific mention is due Dr. Bob Glahn (MDL Director) who is the author of most of the development software, Judy Ghirardelli for LAMP leadership and developing the GEMPAK graphics pre-processing software, Kathy Hughes for developing the MOS thunderstorm equations, and Paul Dallavalle and Jerry Wiedenfeld for general support of the LAMP thunderstorm effort.

Most of the radar reflectivity data used in this study was provided by Global Hydrology Resource Center (GHRC) of the Global Hydrology and Climate Center (GHCC) in Huntsville, Alabama. GHRC received the radar data from Weather Science, Inc. NLDN data were provided by the NASA Lightning Imaging Sensor (LIS) instrument team and the LIS data center via GHRC through a license agreement with Global Atmospherics, Inc (GAI). The data available from the GHRC are restricted to LIS science team collaborators and to NASA EOS and TRMM investigators.

## 8. REFERENCES

Alaka, M. A., W. D. Bonner, J. P. Charba, R. L. Crisci, R. C. Elvander, and R. M. Reap, 1973: Objective techniques for forecasting thunderstorms and severe weather. Final Report, Rep. No. FAA-RD-73-117, Techniques Development Laboratory, National Weather Service, NOAA, U.S. Department of Commerce, 97 pp.

Brier, G. W., 1950: Verification of forecasts expressed in terms of probabilities. *Mon. Wea. Rev.,* **78**, 1-3.

Charba, J. P., 1977: Operational system for predicting thunderstorms two to six hours in advance. NOAA Technical Memorandum NWS TDL-64, National Oceanic and Atmospheric Administration, U.S. Department of Commerce, 24 pp.

____, 1998: The LAMP QPF products. Part I: Model development. *Wea. Forecasting*, **13**, 934-965.

____, F. Liang, 2005: Quality control of gridded national radar reflectivity data. (Manuscript in preparation).

Cummins, K. L., M. J. Murphy, E. A. Bardo, W. L. Hiscox, R. B. Pyle, and A. E. Pifer, 1998. A Combined TOA/MDF Technology Upgrade of the U. S. National Lightning Detection Network, *J. Geophys. Res.*, **103**, 9035-9044.

Glahn, H. R., and D. A. Lowry, 1972: The use of model output statistics (MOS) in objective weather forecasting. *J. Appl. Meteor.*, **11**, 1203–1211.

____, and D. A. Unger, 1986: A Local AFOS MOS Program (LAMP) and its application to wind prediction. *Mon. Wea. Rev.*, **114**, 1313–1329.

____, D. P. Ruth, 2003: The new digital forecast database of the National Weather Service. *Bull. Amer. Meteor. Soc.*, **84**, 195-201.

____, and J. E. Ghirardelli, 2004: The new and improved Localized Aviation MOS Program (LAMP) Analysis and Prediction System. *Preprints 20th Conference on Weather Analysis and Forecasting/16th Conference on Numerical Weather Prediction*, Seattle, WA, Amer. Meteor. Soc., CD-ROM, J12.3.

Hughes, K. K., 2004: Probabilistic lightning forecast guidance for aviation. *Preprints 22th Conference on Severe Local Storms,* Hyannis, MA, Amer. Meteor. Soc., CD-ROM, 2.6.

Iredell, M., and P. Caplan, 1997: Four-times-daily runs of the AVN model. *NWS Technical Procedures Bulletin* No. 442, National Oceanic and Atmospheric Administration, U. S. Department of Commerce, 3pp.